

GRANULAR PRESSURE IN A LIQUID FLUIDIZED BED

V. Zivkovic^{1*}, M. J. Biggs¹, D. Glass²

¹ School of Chemical Engineering, The University of Adelaide, Adelaide, SA, 5005, Australia

² Institute for Materials and Processes, The University of Edinburgh, Sanderson Building, King's Buildings, Mayfield Road, Edinburgh EH9 3JL, UK

*Email: vladimir.zivkovic@adelaide.edu.au

ABSTRACT

The granular pressure and granular temperature underpin various models of granular flows whilst they are playing an increasing role in modelling of other phenomena in granular systems such as heat transfer, segregation, erosion, attrition and aggregation. The development and validation of these theories demand experimental determination of these two quantities. Diffusing wave spectroscopy (DWS) is now an accepted technique for measurement of granular temperature in dense granular systems. Using the kinetic theory of granular flow expression, we have derived for the first time as far as we are aware the granular pressure from DWS data for a liquid fluidized bed. The determined variation of mean granular pressure with solid volume fraction is compared with previously published theoretical models and experimental data of others. Additionally, we report for the first time ever as far as we are aware the variation of the granular pressure with height above the distributor for several mean solids volume fractions.

INTRODUCTION

Collisional particle pressure, or granular pressure, is defined by some as the force exerted by a moving granular medium on the walls of the vessel containing the medium (Campbell & Wang, 1991; Zenit et al., 1997). The particle pressure underpins various granular flow models (Ishii, 1975; Enwald et al., 1996) and is a dominant factor determining the stability of the flow in fluidized beds (Needham & Merkin, 1983; Foscolo & Gibilaro, 1987; Batchelor, 1988).

Campbell and Wang (1991) developed a probe to isolate the particle pressure in a fluidized bed by subtraction between the total and the fluid pressure directly at the point of measurement. This particle pressure transducer is very simple and consists of a solid diaphragm flush-mounted into the wall. The face of the diaphragm experiences the combined pressure of fluid and particles, while the rear experiences only fluid forces as particles are prevented from entering through the access holes into a chamber behind the diaphragm. Campbell and collaborators (Campbell & Wang, 1991; Campbell & Rahman, 1992; Rahman & Campbell, 2002) and others (Polashenski Jr & Chen, 1997; Polashenski Jr & Chen, 1999) measured the particle pressure in gas fluidized beds using this approach. Development of a high-frequency-response pressure transducer capable of detecting changes in pressure lasting up to 2 μ s (Zenit et al., 1997), allowed measurement of particle pressure from individual particle impacts. Pressure fluctuations below 1 kHz are filtered completely so only the pressure pulses generated by the collisions of particles, typically lasting tens of microseconds, are detected (Zenit

V. Zivkovic, M.J. Biggs and D.H. Glass, Granular pressure in a liquid fluidized bed, in the *Proceedings of Chemeca 2010: The 40th Australasian Chemical Engineering Conference*, paper #363 (10 pages). ISBN: 978-085-825-9713.

et al., 1997; Buffière & Moletta, 2000). This approach has been used to measure particle pressure in liquid (Zenit et al., 1997), gas-liquid (Buffière & Moletta, 2000) and vibrated (Falcon et al., 2006) fluidized beds. There is a potential third approach of obtaining the particle pressure experimental data, but it has not been used to our knowledge. Constitutive relation of the kinetic theory of granular flow enables computations of the granular pressure from measurement of the granular temperature and vice versa. This relations was only used for obtaining the granular temperature from particle pressure measurement in gas fluidized bed (Polashenski Jr & Chen, 1997).

Liquid fluidized beds usually expand in homogenous way in contrast to gas fluidized bed, which are generally unstable and give rise to bubbling behaviour. This makes liquid fluidized beds particularly suitable for testing two-phase flow models across a wide range of solid fractions (Gevrin et al., 2008). Yet, there has been only one experimental study of the particle pressure in liquid fluidized bed (Zenit et al., 1997). Zenit et al. (1997) study was very thorough, but they were using relatively large particles which fall in transitional or even bubbling regime (steel particles) of a flow map (Di Felice, 1995) based on the criterion equation of Gibilaro et al. (1990). Even though it was not reported by Zenit et al. (Zenit et al., 1997), a non-homogenous behaviour and even appearance of bubbles can be expected in transitional regime of liquid fluidization which in principle can have influence on the particle pressure. Hence, it is desirable to obtain granular pressure measurement for smaller particles which strictly fall in homogenous regime of liquid fluidization – this is done here.

We report here the granular pressure data for a thin, rectangular bed of small glass particles fluidized by water across a wide range of superficial velocity. The granular temperature data measured by diffusing wave spectroscopy (Zivkovic et al., 2009a) was used to calculate the granular pressure using the kinetic theory of granular flow equations (Gidaspow, 1994; Jackson, 2000). We first outline the experimental details, including an overview of DWS and details pertaining to the apparatus and the particulate material, and the experimental procedure used. This is followed by presentation of the results obtained and their discussion.

EXPERIMENTAL DETAILS

Experimental apparatus

The fluidized bed apparatus is illustrated in Fig. 1a. The main part is a half metre high rectangular bed with a cross-section of 200 mm by 20 mm. It was mounted on a linear stage so that different points of the bed could be investigated with ease. The distributor, which consists of a stainless steel mesh of 40 μm apertures and a 5 cm deep packed bed of 1.5 mm stainless steel beads, was designed to provide highly uniform and homogeneous fluidization. The overflow water at the top of the column was recirculated back into a feed reservoir and a centrifugal pump, forming a closed loop. The liquid flow was measured by a calibrated rotameter (KDG 2000, KDG flowmeters, UK) and temperature of water was maintained at $20 \pm 0.5^\circ \text{C}$. The fluidized particles were small glass particles with density of $\rho_p = 2500 \text{ kg/m}^3$ (SiLibeads type S, Sigmund Lindner, UK). The beads were carefully resieved between two close meshes to obtain narrowly distributed glass beads of diameter $d_p = 165 \pm 15 \mu\text{m}$. The liquid FB was filled with granular material to give a 75 mm defluidized bed height.

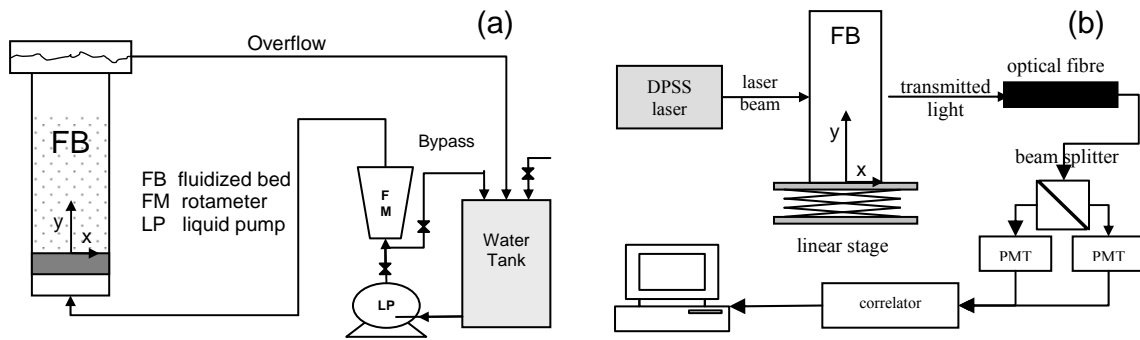


Fig. 1: Schematic diagram of (a) liquid FB apparatus and (b) DWS apparatus.

Diffusing wave spectroscopy (DWS), which is described in detail by Weitz and Pine (1993), is a multiple light scattering technique with high spatiotemporal resolution (1-10 nm, 2 ns). It has been applied in the study of particle dynamics in various dense granular systems (see for example Zivkovic et al., 2009b and reference therein). The DWS apparatus for use in the transmission mode is illustrated in Fig. 1b. A 400 mW diode pumped solid state linearly polarized laser (Torus 532, Laser Quantum Ltd., Cheshire, UK) operating at a wavelength of $\lambda = 532$ nm in single longitudinal mode illuminates one side of the bed at the point of interest with an ~ 2 mm diameter laser beam. The light passes through the medium, scattering many times before exiting the back of the bed as a diffusion spot of ~ 20 mm diameter for our bed of 20 mm thickness. The scattered light was collected over time, t , with a single mode optical fibre (OZ Optics Ltd., Ottawa, Canada). The collected light signal was bifurcated and the 50/50 split light signal fed into two matched photomultiplier tubes (PMTs) to reduce spurious correlation due to possible after-pulsing effects of the detector. The intensity outputs $I(t)$ from the PMTs were amplified and fed to a multi-tau digital correlator (Flex 05, Correlator.com, US), which performed a pseudo cross-correlation analysis in real time to give the intensity autocorrelation function (IACF), $g_2(t)$, that was stored on a PC for further offline analysis as detailed below.

Experimental procedure

Measurement of solid volume fraction

In a steady-state regime of fluidization, the height of the front between fluidized particles and clear fluid at the top of the bed was determined. The height was measured using a measuring tape glued to the side bars of the apparatus with an accuracy of ± 1 mm. By measuring the mean fluidized bed height, h , the mean solids volume fraction, $\langle \phi \rangle$, was then calculated by

$$\langle \phi \rangle = \frac{m_p}{\rho_p Ah} \quad (1)$$

where m_p is the mass of fluidized particles, and A is the cross-sectional area.

The solids volume fraction was also determined as a function of measuring height, y , by measuring the transmitted laser light intensity through the liquid fluidized bed normalized to transmission through a reference sample of the same thickness, I/I_r (Duru et al., 2002; Segrè & McClymer, 2004; Tee et al., 2008). The light intensity was

detected and recorded with a digital optical power meter (Model 815, Newport Corporation, US). The signals were averaged over 60 s, a time much larger than the expected period of any density waves. For calibration we used height averaged values of the transmitted light intensities (Duru et al., 2002) at a fixed mean particle solids volume fraction as it gave slightly better results than mid-height transmitted light intensities, an approach used by Segre and McClymer (2004).

Measurement of granular temperature

A detailed description of the method used to determine the granular temperature in the liquid fluidized bed using DWS is provided in Zivkovic et al (Zivkovic et al., 2009a). We provide here, however, a brief overview. Intensity autocorrelation functions (IACF) were obtained by collecting and correlating ten blocks of data of 30 s long each. Each IACF was then subject to further analysis as follows. The normalized electric-field autocorrelation function (FACF), $g_1(t)$, was obtained from the intensity autocorrelation function, $g_2(t)$, using the Siegert relationship (Berne & Pecora, 1976; Weitz & Pine, 1993)

$$g_2(t) \equiv \frac{\langle I(0)I(t) \rangle}{\langle I \rangle^2} = 1 + \beta_1 |g_1(t)|^2 \quad (2)$$

where β_1 is a phenomenological parameter determined from the intercept of the IACF; this phenomenological parameter was always found to be $\beta_1 \approx 0.5$, as expected. The mean square displacement (MSD) of the particles, $\langle \Delta r^2(t) \rangle$, was determined by inverting the FACF using the formula given by Weitz and Pine (1993)

$$g_1(t) = \frac{\frac{L/l^* + 4/3 \left[\sinh\left(\frac{z_0}{l^*} \sqrt{X}\right) + \frac{2}{3} \sqrt{X} \cosh\left(\frac{z_0}{l^*} \sqrt{X}\right) \right]}{z_0/l^* + 2/3}}{\left(1 + \frac{4}{9} X\right) \sinh\left(\frac{L}{l^*} \sqrt{X}\right) + \frac{4}{3} \sqrt{X} \cosh\left(\frac{L}{l^*} \sqrt{X}\right)}; X = \langle \Delta r^2(t) \rangle k_0^2 + \frac{3l^*}{l_a} \quad (3)$$

where L is the sample thickness (20 mm here), l^* is the transport mean free path, l_a is the absorption path length, $z_0 = \gamma l^*$ is the distance over which the incident light is randomized, and $k_0 = 2\pi/\lambda$ is wave vector of light in the medium. The scaling factor, γ , was set to unity in line with common practice (Weitz & Pine, 1993; Xie et al., 2006).

The square of particle velocity fluctuations about the mean flow velocity can be derived straightforwardly from the ballistic region of the MSD (Menon & Durian, 1997), provided it is resolved, where

$$\langle \Delta r^2 \rangle = \langle \delta v^2 \rangle t^2 \quad (4)$$

The granular temperature for a three dimensional flowing granular material is defined as

$$\theta = \frac{1}{3} \langle \delta v^2 \rangle \quad (5)$$

Equation 3 requires knowledge of the transport mean free path, l^* , or step size in the random walk of photons, and the diffusive absorption path length, l_a , which accounts for light absorption, at the positions and conditions considered. They were determined using the method of static transmission (Weitz & Pine, 1993; Leutz & Rička, 1996) as a function of solid volume fraction and height above the distributor (for more details see Zivkovic et al., 2009a).

Determination of granular pressure

For determination of granular pressure, we used the kinetic theory of granular flow expression (Gidaspow, 1994; Jackson, 2000)

$$P^* = \rho_p \phi \theta [1 + 2\phi g_0(\phi)(1 + e)] \quad (6)$$

where $g_0(\phi)$ is the radial distribution function (RDF), and e is the restitution coefficient. We determined the granular pressure using three common forms of the RDF, namely those proposed by Bagnold (1954)

$$g_0(\phi) = [1 - (\phi / \phi_{\max})^{1/3}]^{-1} \quad (7)$$

Carnahan & Starling (1969),

$$g_0(\phi) = \frac{2 - \phi}{2(1 - \phi)^3} \quad (8)$$

and Lun & Savage (1986),

$$g_0(\phi) = (1 - \phi / \phi_{\max})^{-5\phi_{\max}/2} \quad (9)$$

where ϕ_{\max} is the maximum possible solid volume fraction of the system, which was assumed here to be equal to the random close packing limit of 0.64. The coefficient of restitution was assumed to be $e = 0.95$, which has been suggested previously for glass particles (Lun & Savage, 1986). The slight influence of impact velocity on the restitution coefficient (Lun & Savage, 1986) is expected to be negligible for our range of velocities (order of 1 cm/s).

RESULTS AND DISCUSSION

Granular temperature

Fig. 2(a) shows variation of height averaged granular temperature with superficial velocity. The granular temperature, which is the same order of magnitude as the square of superficial velocity, increases with superficial velocity up to a maximum at $U_0 = 7.5$ mm/s. In order to explain the observed maximum, we re-plot the data to obtain the variation with the mean solid fraction, $\langle \phi \rangle$, as shown in Fig. 2(b). This exhibits a maximum at $\langle \phi \rangle = 0.175$. This is inline with the simulations of Gevrin *et al.* (2008), who reported a maximum in the granular temperature of glass particles at a solid fraction close to $\phi = 0.2$. A similar trend was observed when the local solid fraction was plotted against the local velocity fluctuation data (Zivkovic *et al.*, 2009a), indicating that the granular temperature may be described solely in terms of the solids volume fraction, ϕ , for liquid fluidized beds.

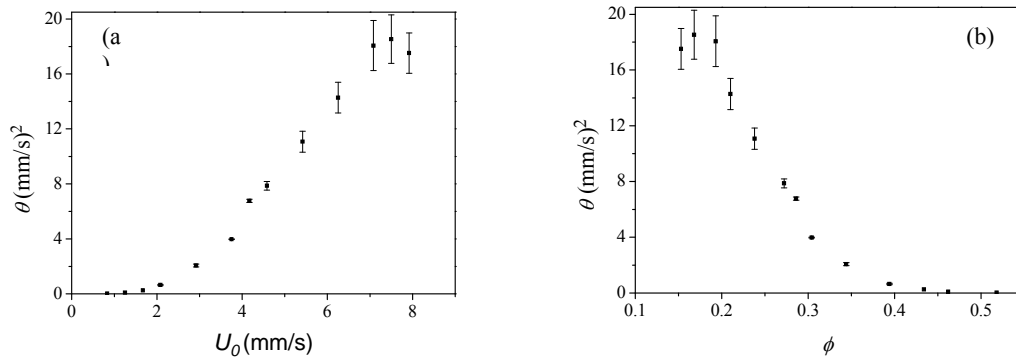


Fig. 2: The variation of height averaged values of granular temperature, θ , with superficial velocity U_0 (a) and with the mean solid volume fraction, ϕ (b). Error bars are standard deviation of height averaged granular temperature data.

Mean granular pressure variation with superficial velocity and mean solid volume fraction

Experimental data shown in Fig. 2(b) was used to calculate the mean granular pressure in the bed using Eq. 6 with the three different forms for radial distribution function (RDF), Eq. 7, 8 and 9. Fig. 3(a), which shows the granular pressure variation with superficial velocity, indicates that whilst the granular pressure obtained from the Bagnold RDF is up to 50% larger than the granular pressure obtained using the other two RDF forms, the trends are very similar. In particular, irrespective of the RDF used, the granular pressure increases rapidly with superficial velocity until it plateaus for some intermediate range of velocities before decreasing as the superficial velocity approaches the particle terminal velocity. This is very similar to the results of Zenit *et al.* (1997), especially for low inertia particles.

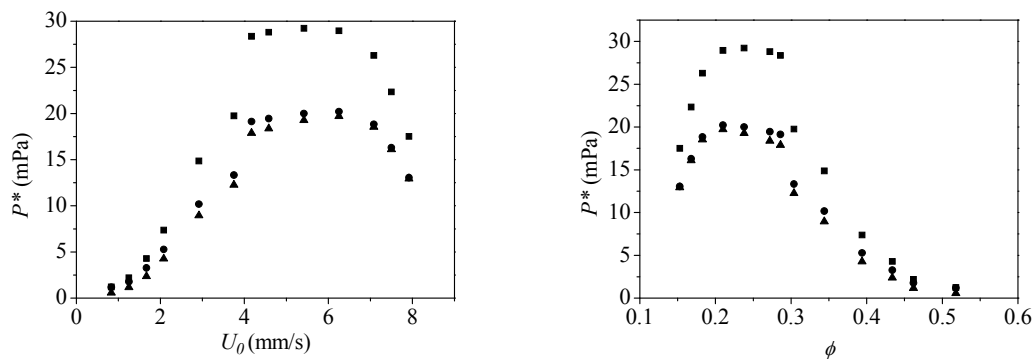


Fig. 3: The mean granular pressure, P^* , as a function of superficial velocity U_0 (a) and the mean solids volume fraction, ϕ (b). The data has been obtained from Eq. 6 using the radial distribution functions proposed by Bagnold (square), Carnahan & Stirling (triangle) and Lun & Savage (circles).

For better comparison, the granular pressure is plotted against the mean solids volume fraction as shown in Fig. 3(b). There is a very little variation of the granular pressure with mean solids volume fraction in maximum plateau region, but the mean granular pressure sharply decreases as mean solids volume fraction approaches both the dilute

and close-packed limits. The maximum granular pressure occurs at intermediate values of the mean solids volume fraction, between 0.2 and 0.3 in our case. This range is at slightly lower than observed by Zenit *et al.* (1997), who observed maxima at solid volume fractions between 0.3 and 0.35, but is inline with their observation that maximum pressure is located at lower solids volume fractions for smaller particles ,i.e. low inertia particles (Zenit *et al.*, 1997).

Fig. 4 compares the maximum particle pressures obtained here against the models proposed by Batchelor (1988), Buyevich & Kapbasov (1999) and Wang & Ge (2005). Whilst the first of these models somewhat under-predicts the results obtained here and presents a maximum at slightly lower solids volume fractions, its shape is otherwise remarkably similar. Both the models of Buyevich & Kapbasov (1999) and Wang & Ge (2005) predict maximum in granular pressure for solid fraction of around 0.45, which is well above that obtained here but inline with that expected for high inertia particles for which they were tailored (Wang & Ge, 2005). Moreover, the simulation results of (Gevrin *et al.*, 2008) are similar to these theoretical models, and accordingly show the greatest discrepancy with the experimental result for low inertia particles (e.g. nylon beads experimental data of Zenit *et al.* (1997)). These results suggest that new theoretical and simulation models are still required.

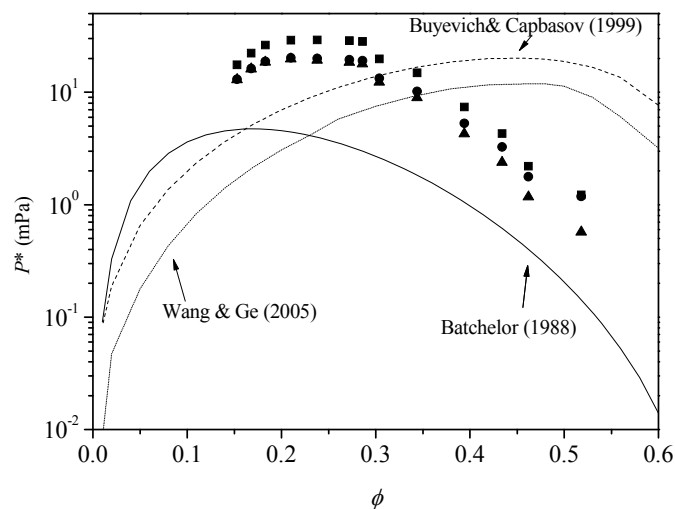


Fig. 4: Comparison of the experimentally results (points) with theoretical models of Batchelor (1988), Buyevich & Kapbasov (1999) and Wang & Ge (2005). Symbols representing the experimental data are as for Fig. 3.

Granular pressure variation with height above the distributor

We used the local solids volume fraction and granular temperature data to obtain, for the first time as far as we are aware, the variation of the solids pressure in a liquid fluidized bed with height above the distributor, Fig. 4. Fig. 5(a) and (b) show that the granular pressure varied little with height above the distributor for mean solids volume fractions above $\langle \phi \rangle = 0.238$. At $\langle \phi \rangle = 0.238$, there appears to be a possibility of a weak variation of granular pressure with height, although the uncertainty in the experimental data means this variation is not certain. This weak variation is perhaps not unexpected, as the mean solids volume fraction lies in the region where the granular pressure

plateaus (*c.f.* Fig. 3(b)). Fig. 5(c) and (d) show that for mean solids volume fractions below $\langle\phi\rangle = 0.238$, there is considerable variation of local particle pressure with height above the distributor. This confirms simulation results of Gevrin et al. (2008) at low solids volume fractions.

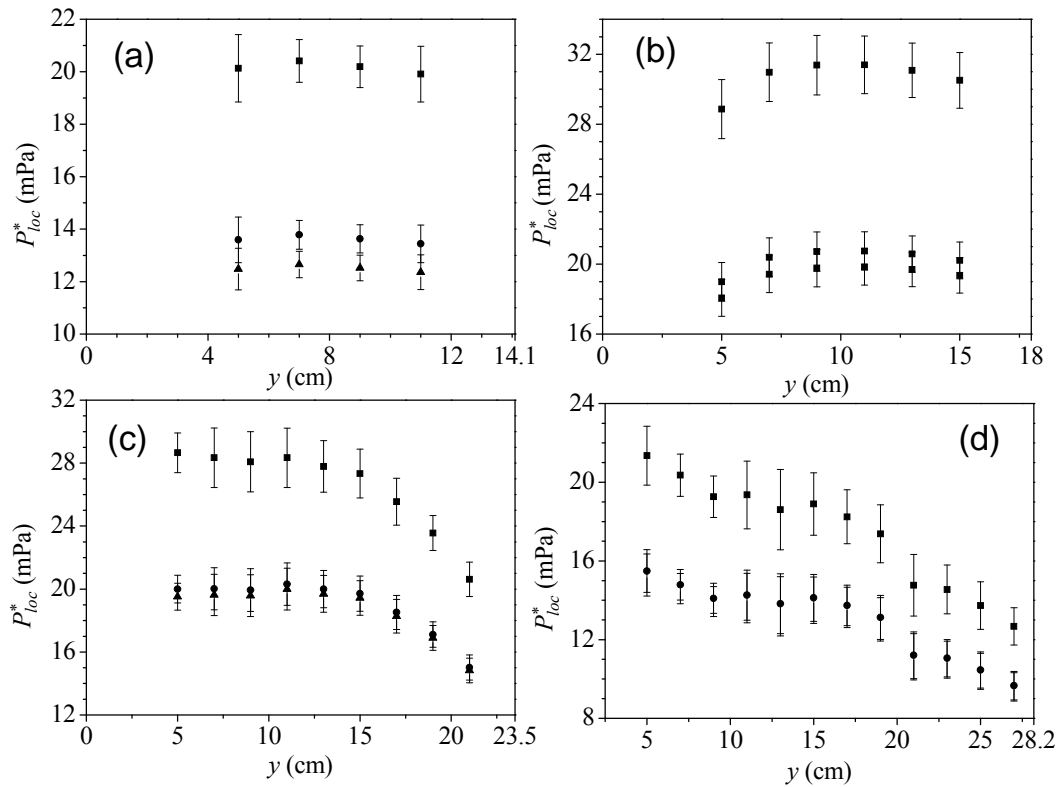


Fig. 5: The local granular pressure, P_{loc}^* , as a function of the height above the distributor, y , for four mean solid volume fractions: (a) $\phi = 0.306$, (b) $\phi = 0.238$ (c) $\phi = 0.183$, and (d) $\phi = 0.153$. The data has been obtained from Eq. 6 using the radial distribution functions proposed by Bagnold (square), Carnahan & Stirling (triangle) and Lun & Savage (circles). The right-hand borders of each plot represent the mean fluidized bed heights, h . Error bars are standard deviation of calculated local granular pressure.

CONCLUSION

Using kinetic theory of granular flow and diffusing wave spectroscopy experimental data, we obtained the granular pressure of $165\ \mu\text{m}$ glass particles in a thin, rectangular water fluidized bed. The derived granular pressure increases with mean solids fraction until it plateaus at intermediate fractions (between 0.2 and 0.3) before decreasing again as the system approaches the close packed limit. This is in line with experimental result of Zenit et al (1997), indicating that DWS is a suitable technique for obtaining granular pressure in fluidized systems. The best agreement is with a theoretical model of Batchelor (1988), while other models (refs) must be adjusted for low inertia particles. For the first time, the granular pressure axial profiles were determined experimentally. Significant variation with height is observed at low solids volume fractions, inline with the simulation results of Gevrin et al. (2008).

REFERENCE

- Bagnold, RA 1954, 'Experiments on a Gravity-Free Dispersion of Large Solid Spheres in a Newtonian Fluid under Shear', *Proceedings of the Royal Society of London. Series A. Mathematical and Physical Sciences*, vol. 225, pp. 49-63.
- Batchelor, GK 1988, 'A new theory of the instability of a uniform fluidized bed', *Journal of Fluid Mechanics*, vol. 193, pp. 75-110.
- Berne, JB & Pecora, R 1976. *Dynamic light scattering*. New York, Wiley-Interscience Publication.
- Buffière, P & Moletta, R 2000, 'Collision frequency and collisional particle pressure in three-phase fluidized beds', *Chemical Engineering Science*, vol. 55, pp. 5555-5563.
- Buyevich, YA & Kapbasov, SK 1999, 'Particulate pressure in disperse flow', *International Journal of Fluid Mechanics Research*, vol. 26, pp. 72-97.
- Campbell, CS & Rahman, K 1992, 'An improved particle pressure transducer', *Measurement Science and Technology*, vol. 3, pp. 709-712.
- Campbell, CS & Wang, DG 1991, 'Particle pressure in gas-fluidized beds', *Journal of Fluid Mechanics*, vol. 227, pp. 495-508.
- Carnahan, NF & Starling, KE 1969, 'Equation of state for nonattracting rigid spheres', *The Journal of Chemical Physics*, vol. 51, pp. 635-636.
- Di Felice, R 1995, 'Hydrodynamics of liquid fluidisation', *Chemical Engineering Science*, vol. 50, pp. 1213-1245.
- Duru, P, Nicolas, M, Hinch, J & Guazzelli, É 2002, 'Constitutive laws in liquid-fluidized beds', *Journal of Fluid Mechanics*, vol. 452, pp. 371-404.
- Enwald, H, Peirano, E & Almstedt, AE 1996, 'Eulerian two-phase flow theory applied to fluidization', *International Journal of Multiphase Flow*, vol. 22, pp. 21-66.
- Falcon, E, Aumaitre, S, Evesque, P, Palencia, F, Lecoutre-Chabot, C, Fauve, S, Beysens, D & Garrabos, Y 2006, 'Collision statistics in a dilute granular gas fluidized by vibrations in low gravity', *Europhysics Letters*, vol. 74, pp. 830.
- Foscolo, PU & Gibilaro, LG 1987, 'Fluid dynamic stability of fluidised suspensions: the particle bed model', *Chemical Engineering Science*, vol. 42, pp. 1489-1500.
- Gevrin, F, Masbernat, O & Simonin, O 2008, 'Granular pressure and particle velocity fluctuations prediction in liquid fluidized beds', *Chemical Engineering Science*, vol. 63, pp. 2450-2464.
- Gibilaro, LG, Di Felice, R & Foscolo, PU 1990, 'Added mass effects in fluidized beds: application of the Geurst-Wallis analysis of inertial coupling in two-phase flow', *Chemical Engineering Science*, vol. 45, pp. 1561-1565.
- Gidaspow, D 1994. *Multiphase Flow and Fluidization — Continuum and Kinetic Theory Descriptions*. San Diego, Academic Press.
- Ishii, M 1975. *Thermo-Fluid Dynamic Theory of Two-phase Flow*. Paris, Eyrolles.
- Jackson, R 2000. *The dynamics of fluidized beds*. New York, Cambridge University Press.
- Leutz, W & Rička, J 1996, 'On light propagation through glass bead packings', *Optics Communications*, vol. 126, pp. 260-268.
- Lun, C & Savage, S 1986, 'The effects of an impact velocity dependent coefficient of restitution on stresses developed by sheared granular materials', *Acta Mechanica*, vol. 63, pp. 15-44.

- Menon, N & Durian, DJ 1997, 'Diffusing-wave spectroscopy of dynamics in a three-dimensional granular flow', *Science*, vol. 275, pp. 1920-1922.
- Needham, DJ & Merkin, JH 1983, 'Propagation of a voidage disturbance in a uniformly fluidized bed', *Journal of Fluid Mechanics*, vol. 131, pp. 427-454.
- Polashenski Jr, W & Chen, JC 1997, 'Normal solid stress in fluidized beds', *Powder Technology*, vol. 90, pp. 13-23.
- Polashenski Jr, W & Chen, JC 1999, 'Measurement of particle phase stresses in fast fluidized beds', *Industrial and Engineering Chemistry Research*, vol. 38, pp. 705-713.
- Rahman, K & Campbell, CS 2002, 'Particle pressures generated around bubbles in gas-fluidized beds', *Journal of Fluid Mechanics*, vol. 455, pp. 103-127.
- Segrè, PN & McClymer, JP 2004, 'Fluctuations, stratification and stability in a liquid fluidized bed at low Reynolds number', *Journal of Physics Condensed Matter*, vol. 16, pp.
- Tee, SY, Mucha, PJ, Brenner, MP & Weitz, DA 2008, 'Velocity fluctuations in a low-Reynolds-number fluidized bed', *Journal of Fluid Mechanics*, vol. 596, pp. 467-475.
- Wang, J & Ge, W 2005, 'Collisional particle-phase pressure in particle-fluid flows at high particle inertia', *Physics of Fluids*, vol. 17, pp. 1-3.
- Weitz, DA & Pine, DJ 1993, *Diffusing-wave spectroscopy. Dynamic Light Scattering: The Method and Some Applications*, W. Brown. Oxford, Clarendon Press, pp. 652-720.
- Xie, L, Biggs, MJ, Glass, D, McLeod, AS, Egelhaaf, SU & Petekidis, G 2006, 'Granular temperature distribution in a gas fluidized bed of hollow microparticles prior to onset of bubbling', *Europhysics Letters*, vol. 74, pp. 268-274.
- Zenit, R, Hunt, ML & Brennen, CE 1997, 'Collisional particle pressure measurements in solid-liquid flows', *Journal of Fluid Mechanics*, vol. 353, pp. 261-283.
- Zivkovic, V, Biggs, MJ, Glass, DH, Pagliai, P & Buts, A 2009, 'Granular temperature in a liquid fluidized bed as revealed by diffusing wave spectroscopy', *Chemical Engineering Science*, vol. 64, pp. 1102-1110.
- Zivkovic, V, Biggs, MJ, Glass, DH & Xie, L 2009, 'Particle dynamics and granular temperatures in dense fluidized beds as revealed by diffusing wave spectroscopy', *Advanced Powder Technology*, vol. 20, pp. 227-233.